Review _____ *Forma*, **19**, 335–354, 2004

Growth in Plants: A Study in Number

Jay KAPPRAFF

New Jersey Institute of Technology, Department of Mathematics, Newark, NJ 07102, U.S.A.
E-mail address: kappraff@verizon.net

(Received March 11, 2005; Accepted March 18, 2005)

Keywords: Phyllotaxis, Fibonacci Numbers, Golden Mean, Continued Fractions, Farey Series, Wythoff's Game, Zeckendorf Notation

Abstract. Three models of plant phyllotaxis are presented. Phyllotaxis is shown to be governed by subtle properties of number which insure that the florets are arranged so as to have the most space and therefore have the greatest access to sunlight. The mathematical tools discussed are Farey series, Wythoff's game, continued fractions, and a Fibonacci number system called Zeckendorf notation.

1. Introduction

Many scientists and keen observers of nature such as the architect Le Corbusier and the composer Bela Bartok have observed the elaborate spiral patterns of *stalks*, or *parastiches*, as they are called, on the surface of pine cones, sunflowers, pineapples, and other plants. It was inevitable that the symmetry and order of plants so evident to the observer and so evocative of sentiment to the artist and poet should become a source of mathematical investigation.

ADLER (1997), a pioneer in modern theories of plant growth, or plant phyllotaxis as it is called, has studied the history of this subject. Adler has traced the general observation of the regular spacing of leaves as far back as Theophrastus (370 B.C.–285 B.C.) and Pliny (25 A.D.–79 A.D.). Leonardo Da Vinci (1452–1519) observed the spiral patterns of plants, while Johannes Kepler (1571–1630) conjectured that *Fibonacci numbers* were somehow involved in the structure and growth of plants. Schimper (1836) observed that after some number of complete turns around the stem of a plant, another leaf lies almost directly above the first. He gave the name *divergence angle* to the number of turns divided by the number of leaves in a cycle. The Bravais brothers (1937) first discovered that the angle between successive stalks in the growth of a plant, the divergence angle, is in most plants $2\pi/\tau^2$ radians or 137.5 degrees where $\tau = (1+\sqrt{5})/2$, is the golden mean.

The stalks or florets of a plant lie along two nearly orthogonal intersecting spirals, one clockwise and the other counterclockwise. The numbers of counterclockwise and clockwise spirals on the surface of the plants are generally successive numbers from the F-series: 1, 1, 2, 3, 5, 8, ..., and such growth is known as *normal phyllotaxis*. However, successive

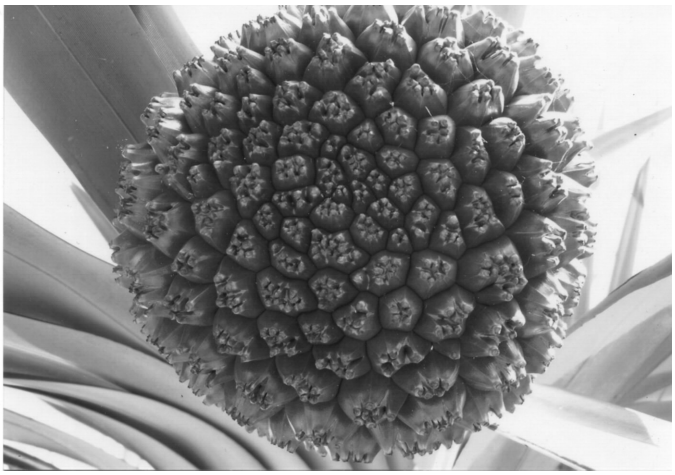

Fig. 1. A plant exhibiting 5,8-phyllotaxis.

numbers from other Fibonacci sequences have been observed such as the *Lucas sequence*: 1, 3, 4, 7, 11, ..., with correspondingly different divergence angles referred to as *abnormal phyllotaxis*. These successive numbers are called the *phyllotaxis numbers* of the plant. For example, there are 55 clockwise and 89 counterclockwise spirals lying on the surface of some sunflowers thus sunflowers are said to exhibit 55,89-phyllotaxis. On the other hand, the plant shown in Fig. 1 has 5,8-phyllotaxis as does the pineapple (although since 13 counterclockwise spirals are also evident on the surface of a pineapple, it is sometimes referred to as 5,8,13-phyllotaxis).

This article will explore the relationship between number and phyllotaxis. The infinite Farey tree and continued fractions will be related to a hierarchy of phyllotaxis numbers. Two equivalent models of plant growth introduced by COXETER (1953, 1961) and VAN ITERSON (1907) will be described. Each model makes use of the fact that florets are arranged so as to "have the most space." Spacing properties of florets will be related to the golden mean. A simplified model of phyllotaxis due to KAPPRAFF (2002) and KAPPRAFF *et al*. (1997) will be described, showing the relationship of this subject to dynamical systems on a torus.

To this day, the physical processes involved in phyllotaxis are a mystery. In this chapter we ignore physical processes, and give only fleeting reference to the geometry of plant growth, in order to underscore the number relationships that lie at the basis of this subject.

2. Coxeter's Model

In Fig. 2, COXETER (1953) transforms the pineapple to a semi-infinite cylinder which has been opened up to form a period strip (meaning that the left and right sides of the rectangle are identified). Notice the three families of spirals. Also notice that the stalks are

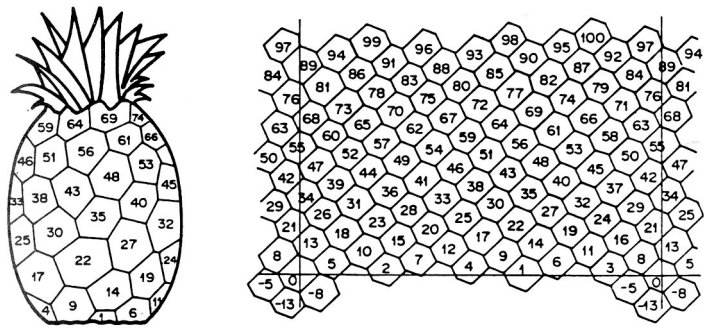

Fig. 2. A pineapple transformed to a semi-infinite cylinder by H. S. M. Coxeter.

labeled chronologically, according to the order in which they appear in the growth process. The center of each stalk makes up a lattice of points which are successively numbered along another *generative spiral*. Each stalk is defined as the set of points nearer to that lattice point than any of the other centers, what in mathematics is known as a *Dirichlet domain* (*D-Domain*). In general, the Dirichlet domains of a lattice are hexagons, although at certain critical points they become rectangles. Since the 5th, 8th, and 13th stalk (hexagon) border the initial stalk (labeled 0), this diagram represents 5,8,13-phyllotaxis. In the most prevalent form of phyllotaxis, the center of each stalk occurs at an angle $\lambda = 2\pi/\tau^2$ radians or 137.5 degrees displaced from the preceding one where λ is the *divergence angle*. Other forms of phyllotaxis have been observed with anomalous angles related to other *noble numbers* as described Appendix A.

The lattice points also rise as if moving along a slightly inclined ramp by an amount called the *pitch*. If the pitch is less steep, then larger numbered stalks will border the initial stalk giving rise to larger phyllotaxis numbers. Notice that a sequence of stalks alternates on either side of the initial stalk numbered by q_k from the Fibonacci series. This is a consequence of the properties of the convergents p_k/q_k

$$1/3,\ 2/5,\ 3/8,\ 5/13,\ \ldots$$

of the continued fraction expansion of $1/\tau^2 = 1/2 + 1/1 + 1/1 + 1/1 \ldots$ The *convergents* are the rational numbers obtained by truncating the continued fraction at successive levels. Appendix A gives a brief discussion of continued fractions. The next closest approach, the q_k-th point, to the zero point occurs after the entire series has rotated p_k times about the cylinder. This is the result of the fact that the continued fraction expansions of $1/\tau$ and $1/\tau^2$ have no *intermediate convergents* (see Appendix A). For example, in Fig. 2, the 13th stalk occurs after 5 revolutions around the stem of the pineapple. Since p_k/q_k is the k-th convergent to $1/\tau^2$ in its continued fraction expansion, it follows (see KAPPRAFF, 2002) that stalk q_k occurs after p_k revolutions about the cylinder, and

$$\lambda q_k - 2\pi p_k \approx 0 \quad \text{where } \lambda = 2\pi/\tau^2. \tag{1}$$

3. Van Iterson's Model

Van Iterson's *cylindric model* is similar to Coxeter's model, however, it is easier to analyze. VAN ITERSON (1907) and PRUSINKIEWICZ and LINDENMAYER (1990) uses tangent circles to model the florets as shown in Fig. 3 for *m*,*n*-phyllotaxis. A clockwise spiral rises from the origin in increments of *m* florets while a counterclockwise spiral rises in increments of *n* florets, both spirals intersecting at the *mn*-th floret. Also floret numbers *m* and *n* are both tangent to the initial floret labeled, 0. Fig. 4 illustrates this 2,3,5-, 3,5-, 3,5 8-, and 5,8-phyllotaxis.

Notice in Fig. 4a that for 2,3,5-phyllotaxis, floret number 2, 3, and 5 are tangent to the initial floret, 0. As the floret diameter d decreases, the lattice undergoes a transformation from one set of phyllotaxis numbers to another. As shown in Fig. 4, and on the phyllotaxis

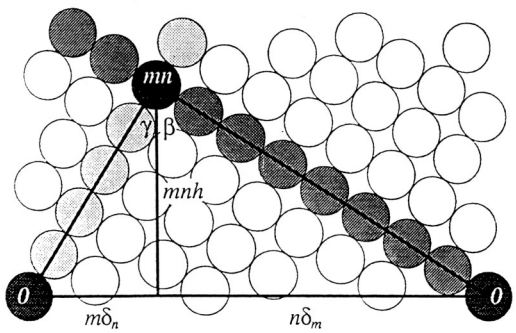

Fig. 3. An opposite parastichy triangle (as in ERICKSON (1983)). The base is formed by the circumference of the cylinder. The sides are formed by the parastiches.

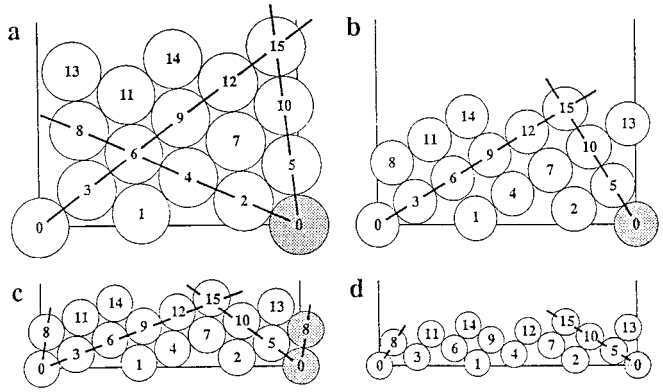

Fig. 4. Patterns of tangent circles drawn on the surface of a cylinder as a function of circle diameter.

tree of Fig. 5, 2,3,5-phyllotaxis is a transition point at which the 2,3-branch of the phyllotaxis tree bifurcates to 2,5-and 3,5-phyllotaxis. The divergence angles at general transition points, $m,n,m+n$-phyllotaxis are shown in Fig. 5. At a transition point each circle is tangent to six circles in a close-packed arrangement (see Figs. 4a and c). Also angle $\gamma+$

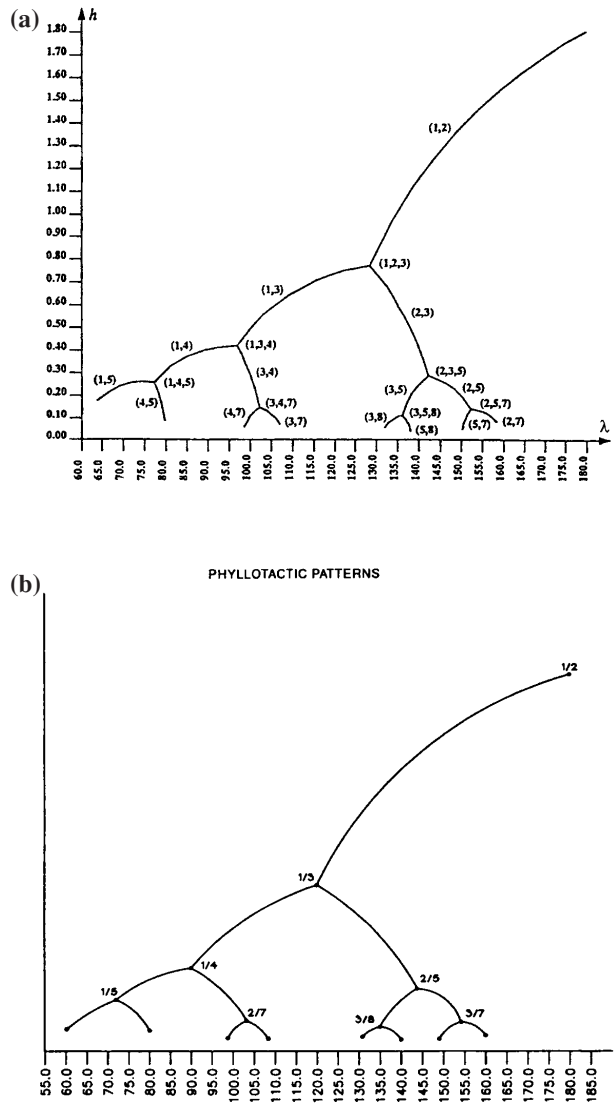

Fig. 5. (a) The vertical displacement h as a function of the divergence angle λ and for various phyllotatic patterns (m, n); (b) A global picture showing the relationship between Farey sequences and divergence angles. Each $0 \le p/q \le 1/2$ corresponds to an angle $360 \times (p/q)$ degrees. Number pairs on the edges refer to phyllotaxis numbers.

β in Fig. 4 becomes 120 deg., and a third spiral becomes evident as shown in Figs. 4a and c.

Van Iterson used his model to compute the pitch h, measured as the distance between any two successive lattice points, the divergence angle λ, and the phyllotaxis numbers m, n. He then determined the relationship between these quantities, illustrated by the phyllotaxis tree in Fig. 5a. The positions of the vertices are slightly altered from Fig. 5b, derived from the infinite Farey tree (see Appendix A) and located at angles equal to numbers from the infinite Farey tree between 0 and 1/2 multiplied by 360 degrees, i.e., angles between 0 and 180 degrees. If m, n is interpreted as m/n, you will notice in Fig. 5a that the phyllotaxis numbers are also arranged according to the Farey tree of Table 5b, but with the numbering of its branches reordered. So we see that without the benefit of a geometric model, both the hierarchy of phyllotaxis numbers and the values of the divergence angles are represented by considerations of number only, as demonstrated by KAPPRAFF *et al*. (1997) and KAPPRAFF (2002).

Figures 5a and b also show that any pair of phyllotaxis numbers is consistent with a limited range of divergence angles, the angles between the transition points at both ends of the appropriate branch of the phyllotaxis tree. For example, in Fig. 5a, 2,3-phyllotaxis is consistent with angles between 128.5 deg. and 142.1 deg. or, correspondingly in Fig. 5b, to angles between 120 deg. and 144 deg. Also the diameter of the floret circle d decreases for higher phyllotaxis angles. Furthermore h and d at the bifurcation points can be uniquely determined from the phyllotaxis numbers m, n by simple geometry as shown in PRUSINKIEWICZ and LINDENMAYER (1990).

Any relatively prime pair of integers can serve as phyllotaxis numbers, and all such possibilities are arranged in the Farey tree depicted in Figs. 5a and b. Each branch in Figure 5a corresponds to a pair of phyllotaxis angles gotten by zig-zagging left-right or right-left down the tree from that branch according to the sequence LRLRLR ... or RLRLRL ... These phyllotaxis angles correspond to the *noble numbers* described in Appendix A. Further details are found in KAPPRAFF (2002) and MARZEC and KAPPRAFF (1983).

4. Optimal Spacing

The question remains as to why divergence angles are related to the golden mean. Wherever numbers or other quantities are to be evenly distributed in space, the golden mean quite naturally makes its appearance (see Appendix B). The following spacing theorem appears to lie at the basis of why the golden mean arises naturally in the growth of plants and other biological systems.

Theorem 1: Let x be any irrational number. When the points $[x]_f$, $[2x]_f$, $[3x]_f$, ..., $[nx]_f$ are placed on the line segment [0,1], the $n + 1$ resulting line segments have at most three different lengths. Moreover, $[(n+1)x]_f$ will fall into one of the largest existing segments ($[\ ]_f$ means "fractional part of").

It turns out that segments of various lengths are created and destroyed in a first-in-first-out manner. Of course some irrational numbers are better than others at spacing intervals evenly. For example, an irrational number that is near 0 or 1 will start out with

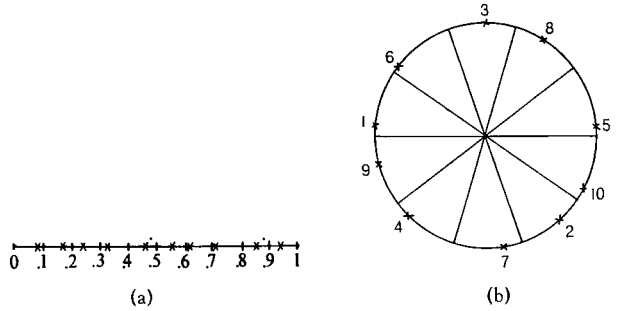

Fig. 6. The points $[n/\tau]_f$ for n = 1, 2, 3, ..., 10 are evenly spaced on the unit interval; (b) the points $2\pi n/\tau$ mod 2π are evenly spaced on the circumference of a circle.

many small intervals and one large one. The two numbers $1/\tau$ and $1/\tau^2$ lead to the "most uniformly distributed" sequence among all numbers between 0 and 1 as demonstrated by MARZEC and KAPPRAFF (1983). These numbers section the largest interval into the golden ratio $1:\tau$.

Theorem 1 is illustrated in Fig. 6a for a sequence of points $[n/\tau]_f$ for n = 1 to 10. This is equivalent to placing the points $2\pi n/\tau^2$ (mod 2π), for n = 1 to 10, around the periphery of a circle as shown in Fig. 6b.

Alternatively, consider the sequence for different values of n of $[n/\tau]_f$:

1 – 0.618, 2 – 0.236, 3 – 0.854, 4 – 0.472, 5 – 0.090, 6 – 0.708, 7 – 0.326, ...

Next, consider subsequences of 1, 2, 3, ... values of $[n/\tau]_f$ and arrange them in order of increasing fractional parts:

1
2 1 (since .236 then .618 is the ordering of fractional parts)
2 1 3 (since .236, .618, .854 is the ordering)
2 4 1 3 (since .236 .472 .618 .854 is the ordering)
5 2 4 1 3
5 2 4 1 6 3
5 2 7 4 1 6 3.

For each subsequence, as a consequence of the Theorem 1, the sum of the differences is a maximum. For example if the integers 1, 2, 3, 4, 5 are arranged on the circumference of a circle in the order 52413, the sum of their differences are 12 and is maximal for all permutations of the integers from 1 to 5. KIMBERLING (A054065) has studied the combinatorics of the sequence obtained by adjoining these subsequences in SLOANE. The implications of this spacing property will be explored further in the next section.

If the center of mass of each stalk of a plant is projected onto the base of the period rectangle in the case of Coxeter's and Van Iterson's models, then the next stalk divides the

Fig. 7. The cross section of a celery plant showing successive stalks evenly placed about the periphery.

largest of the three intervals predicted by Theorem 1 in the golden section $(1:\tau)$. Any other divergence angle would place stalks too near the directions of other stalks and therefore make the stalks less than optimally spaced. However, the divergence angle $2\pi/\tau^2$ leads to the most uniformly distributed set of stalks. For example, the cross section of a celery plant is illustrated in Fig. 7. The centers of mass of successive stalks are numbered. If the positions of these centers are projected onto a circle, they are found to closely match the points shown in Fig. 6b. We see that golden mean divergence angles ensure that successive stalks are inserted at positions on the surface of the plant "where they have the most room."

5. The Gears of Life

In order to gain a clearer understanding of how a single number, the golden mean, operates as a coordinator of space in the natural world, consider a very much simplified mathematical model of plant phyllotaxis that nevertheless encompasses its essence. Figure 8a shows a number wheel with the numbers 1 through 5 placed on its rim. The numbers are arranged clockwise every 72 deg., i.e., 360/5 degrees, beginning with 5 at the apex. Begin at the number 3 and progress clockwise three spaces on the number wheel (or two spaces counterclockwise) to reach 1, and three spaces again to 4, 2, 5, and ending the cycle at 3. The sequence of moves is indicated by the star pentagon {5/3}. Notice that in order to complete a cycle of the five vertices of the star requires a rotation twice around the circle. So we have obtained Adamson's *Primary Phyllotaxis Sequence* (PPS) KAPPRAFF (2002) in the following order:

$$\begin{array}{ll} \text{Floret number } y\text{:} & 3\ 1\ 4\ 2\ 5 \\ \text{Order number } x\text{:} & 1\ 2\ 3\ 4\ 5. \end{array} \qquad (2)$$

The relationship of this wheel to Coxeter's phyllotaxis model in Fig. 2 is revealed when the floret number is graphed as the y coordinate and the order number as the x-coordinate as shown in Fig. 8b with the floret number listed on the graph.

Figure 8b should be visualized as a square in which the bottom and top sides have been *identified* (meaning that when a point passes through the top edge of the square, it enters

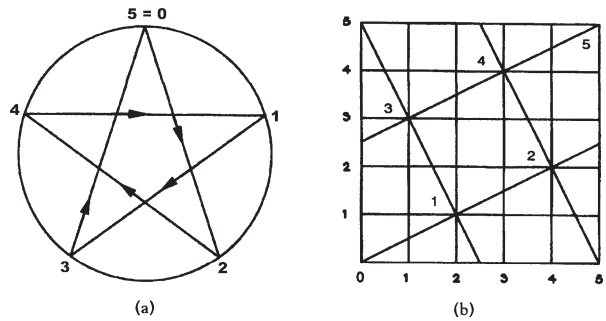

Fig. 8. (a) A number wheel with the numbers 1 through 5 on the rim. Beginning at 3 and progressing counterclockwise successively 2 units results in Adamson's Primary Phyllotaxis Sequence (PPS) graph for five florets graphed on a period torus in (b).

the bottom edge; top and bottom are considered to be identical) and the left and right sides have been identified. In other words Fig. 8b represents a *torus* or rubber tire which has been cut open into a *period rectangle*. On a torus one can trace two distinct cycles shown by the two pairs of lines in Fig. 8b. If each interval on the x-axis corresponds to 360/5 = 72 degrees, then successive floret numbers are counterclockwise from each other by an angle of (2/5)360 = 144 deg., which is an approximation to the phyllotaxis angle of 137.5 deg. A counterclockwise spiral making two turns on the surface of the torus is shown intersecting florets (1, 3, 5) on the first turn and (2, 4) on the second. No consideration has been given to the pitch of the spiral so that this diagram merely shows the relative ordering of the florets, not their proximity to other florets as in Fig. 2.

The dynamics of this simplified model of plant phyllotaxis can also be represented by a pair of gears which prompts me to use the metaphor, "gears of life." One gear has two teeth while the other has five. The gear with five teeth must have a diameter 5/2 times the one with two teeth in order to accommodate the greater number of teeth. Five turns of the small gear in a clockwise direction results in two turns of the large gear in a counterclockwise direction. Musically, this is equivalent to two drums playing with a rhythm in which two beats of one match five beats of the other. Another model which emphasizes this pair of cycles is a torus in which a cycle of five turns in one direction around the torus is completed simultaneous to two turns in the other direction.

The same dynamics which we have described for a wheel with five numbers can be repeated for a gear with any Fibonacci number of teeth, for example the primary phyllotaxis series for a gear with 34 teeth. Beginning on point 21 and progressing 13 spaces on the number wheel, one obtains Sequence 3 for a gear with 34 spokes, the equivalent of Sequence 2 for a gear with 5 spokes which also corresponds to the star polygon {34/21}:

```
21  8 29 16  3 25 11 32 19  6 27 14  1 24  9 30 17  4 25 12 33
 1  2  3  4  5  6  7  8  9 10 11 12 13 14 15 16 17 18 19 20 21
 H  L  H     L        H              L                       H
20  7 28 15  2 25 10 31 18  5 26 13 34=0
22 23 24 25 26 27 28 29 30 31 32 33 34
                                    L
```

(3)

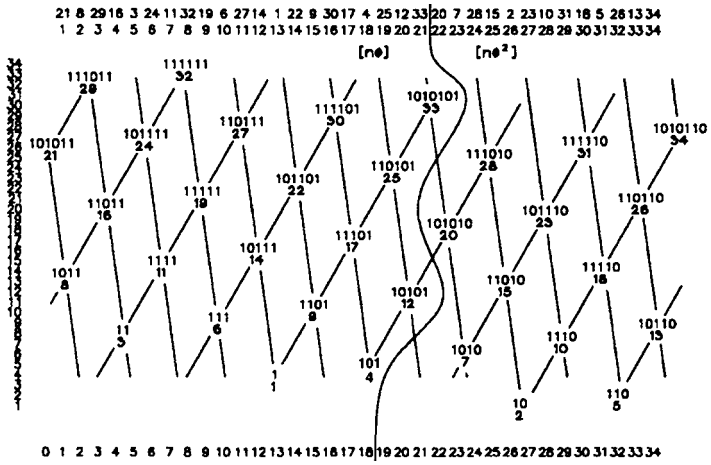

Fig. 9. The PPS graph on a period torus for 34 florets. The line drawn through the figure divides Zeckendorf code representation of floret number ending with 1 from those ending with 0.

The divergence angle between successive florets in a counterclockwise direction is now (13/34)360 = 137.54 degrees, which is an even closer approximation to the phyllotaxis angle.

The PPS graph on a period torus is shown in Fig. 9 with a counterclockwise spiral (solid line) making 13 turns on the surface of the torus and, on each successive turn, intersecting points: (1, 14, 27), (6, 19, 32), ..., (4, 17, 30), (9, 22, 1). A second clockwise spiral is shown approximating one that encircles the torus 8 times. The pair of spirals comprise a schematic diagram of 8, 13-phyllotaxis.

Notice at the bottom of Fig. 9 can be found the same relative ordering of the points 1, 2, 3, 4, 5 that appears in Fig. 8. In a similar manner, the same relative ordering for the diagrams corresponding to wheels with 3, 5, 8, 13, and 21 numbers can be found in Fig. 9. This self-similarity, inherent in the growth process, is a manifestation of the self-similarity inherent in the golden mean. A corresponding wheel unrelated to the golden mean would result in an entirely different PPS diagram for each new wheel. So long as $2\pi/\tau^2$ lies in the interval, $[p_k/q_k, p_{k-1}/q_{k-1}]$ or $[p_{k-1}/q_{k-1}, p_k/q_k]$, then the stalks corresponding to the *gear* with q_k spokes will have the same qualitative ordering. This is an example of a phenomenon called *mode locking* described by KAPPRAFF (2002).

Other interesting properties of the PPS sequence are:

i. The first 21 numbers of this sequence correspond to $[n\tau]$ while the last 13 numbers correspond to $[n\tau^2]$ the two classes of Wythoff pairs (see Appendix C), where $[x]$ signifies "the integer part of x."

ii. Proceeding from left to right, notice that the running high (H) and low (L) values of the floret numbers occur at order numbers corresponding to the Fibonacci numbers. This is a consequence of the property that the continued fraction expansion of the golden mean has no intermediate convergents (see Appendix A) .

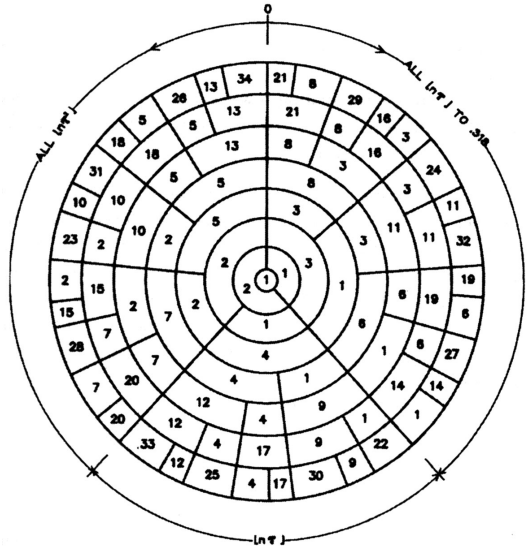

Fig. 10. Adamson's Primary Phyllotaxis Wheel.

iii. If the floret numbers are written in *Zeckendorf notation* (see Appendix D), all of the $[n\tau]$ end in 1 while the $[n\tau^2]$ end in 0, a fact that was also illustrated by Adamson's Wythoff Wheel of Fig. C1. For that matter, notice that identical sequences of digits in Zeckendorf notation are grouped together, another manifestation of self-similarity.

iv. The *rabbit sequence* (see Appendix D): 101101011011 ... is replicated by the last digit of the Zeckendorf notation of the sequence: 1, 2, 3, 4, ... KAPPRAFF (2002) has shown that this sequence is indicative of chaos KAPPRAFF (2002). The rabbit sequence was also described by Kauffman in another article in this issue.

v. The PPS sequence corresponds to a situation in which the positions of all 34 florets are projected onto the x-axis. The differences between adjacent floret numbers of this series are 13 21 13 13 21 13 ..., equivalent to the rabbit Sequence.

The relationship between the numbers of the PPS series is summarized on Adamson's Primary Phyllotaxis Wheel shown in Fig. 10. Here the numbers are arranged around a circle.

The properties of this wheel are:

i. The distribution of numbers around each circle is the most equitable. In fact, the wheel is a discrete replica of the distribution of the numbers $2\pi n/\tau^2$ around the circle in Fig. 6b.

ii. The Fibonacci numbers descend the central radial line, alternating on either side of it, just as in the phyllotaxis lattice (see Fig. 2). Notice how each Fibonacci number originating in the outer circle descends to meet this central Fibonacci series.

iii. Each circle contains the numbers of a PPS sequence alternating clockwise and clockwise, e.g. clockwise for 34-PPS and counterclockwise for 21-PPS, etc.

iv. The depth of the lines radiating towards the center of the concentric circles follows the sequence of the Fibonacci counterpart of the Towers of Hanoi Sequence described in Appendix 3D.

The phyllotaxis diagram in Fig. 2 is the result of considering an infinite number of PPS series. The major difference between this figure and the discrete version of phyllotaxis is that the phyllotaxis spirals are not periodic. Instead of a single spiral that encircles the torus with F_n turns, we now have F_n distinct spirals that encircle the torus but do not close up. The spirals are *quasi-periodic*. It can be shown that plant phyllotaxis is an example of chaos in the spatial rather than the time dimension KAPPRAFF (2002).

6. Conclusion

Plant phyllotaxis has been studied for more than one hundred years. It has stimulated research in biochemistry, botany, horticulture, and mathematics. It appears that plants apportion space so that each stalk has equal access to light and other resources. In order to accomplish this task, plants exhibit an elaborate numerology.

Without the hint of a physical mechanism, or even the artifice of a geometric model, the essentials of the growth process are still manifested through the infinite Farey tree and continued fractions, Wythoff's game as depicted in Adamson's wheels, and the symbolic dynamics of the rabbit tree and series. Without even the concept of pitch or divergence angle, the Farey sequence reveals the relationship between these quantities in remarkable detail, and it even permits us to compute all possible divergence angles observed on actual plants. Without the concept of a lattice of florets, the primary phyllotaxis system (PPS) reveals the ordering of florets into spiral arrangements. We are led into a Platonic mode of thought in which the concepts of number, existing entirely within the mind, can be seen in the plant world.

Decoupling phyllotaxis from science and geometry suggests that this number-theoretical structure is universal and manifests itself in other biological processes and dynamical systems (see KAPPRAFF *et al*., 1997) For this reason, I have given the PPS the name "gears of life." Can a relationship between phyllotaxis and other biological processes be demonstrated?

This article was edited and reprinted from *Beyond Measure: A Guided Tour through Nature, Myth, and Number* by Jay Kappraff. It appeared in the *Knots and Everything Series*, ed. Louis H. Kauffman published by World Scientific (2002).

Appendix A. Continued Fractions and the Infinite Farey Tree

Any positive real number can be expressed as a continued fraction of the form,

$$\alpha = a_0 + \cfrac{1}{a_1 + \cfrac{1}{a_2 + \cfrac{1}{\cdot}}} = \left[a_0; a_1 a_2 a_3 \ldots a_k \ldots\right] = a_0 + 1/a_1 + 1/a_2 + 1/a_3 + 1/\ldots$$

where the indices a_0, a_1, a_2, a_3 ... are positive integers and the latter expression is a shorthand for the continued fraction. If α is a number between 0 and 1 then the leading integer can be eliminated.

Consider a real number $0 < \alpha < 1$ expressible as a continued fraction. The convergents, obtained by truncating the continued fraction at the k-th position, are given by p_j/q_j for j = 1, 2, 3, ..., k, i.e.,

$$a_1\ a_2\ a_3 \ldots \ldots\ a_{k-1}\ a_k$$

$$\frac{p_1}{q_1}\ \frac{p_2}{q_2}\ \frac{p_3}{q_3}\cdots\frac{p_{k-1}}{q_{k-1}}\ \frac{p_k}{q_k}$$

where

$$\frac{p_1}{q_1}=\frac{1}{a_1},\quad \frac{p_2}{q_2}=\frac{a_2}{a_2q_1+1},\quad \frac{p_3}{q_3}=\frac{a_3p_2+p_1}{a_3q_2+q_1},\quad \frac{p_k}{q_k}=\frac{a_kp_{k-1}+p_{k-2}}{a_kq_{k-1}+q_{k-2}}\ \text{ for }\ k\geq 3. \qquad \text{(A1)}$$

Also

$$\frac{p_{k-1}}{q_{k-1}}-\frac{p_k}{q_k}=\frac{(-1)^k}{q_{k-1}q_k}\ \text{ or }\ M=p_{k-1}q_k-p_kq_{k-1}=(-1)^k.$$

The latter expression defines the *modulus*, M, of the pair of rationals, p_{k-1}/q_{k-1} and p_k/q_k. We can see that for any pair of consecutive convergents, $M = \pm 1$. Applying this to 17/47 = [2,1,3,4] one gets the following sequence of convergents:

$$\begin{array}{cccc} 2 & 1 & 3 & 4 \\ 1/2 & 1/3 & 4/11 & 17/47. \end{array} \qquad \text{(A2)}$$

Notice that the modulus between any pair of convergents is $M = \pm 1$.

Given a pair of positive rational numbers, a/b and c/d, the fraction $(a+c)/(b+d)$ lies between them. Therefore corresponding to a pair of successive *convergents*, p_{k-2}/q_{k-2} and p_{k-1}/q_{k-1} there exists a sequence of rational numbers called intermediate fractions defined by,

$$\frac{p_{k-2}}{q_{k-2}},\ \frac{p_{k-2}+p_{k-1}}{q_{k-2}+q_{k-1}},\ldots,\ \frac{p_{k-2}+a_kp_{k-1}}{q_{k-2}+a_kq_{k-1}}=\frac{p_k}{q_k}.$$

It follows when $a_k = 1$, there are no *intermediate convergents* between p_{k-2}/q_{k-2} and p_{k-1}/q_{k-1}.

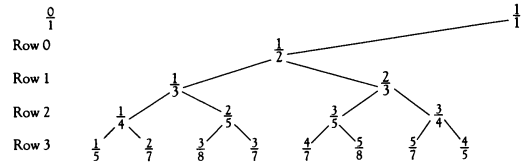

Fig. A1. The infinite Farey tree.

Starting with 0/1 and 1/1, all of the rational numbers in a natural hierarchy can be listed in what is known as an infinite *Farey tree*. For example the next number in the hierarchy is formed by "adding" the pair of adjacent rationals in a way forbidden to children; numerators are added and the denominators are added. For example,

$$\frac{1}{2} = \frac{0}{1} \pm \frac{1}{1} = \frac{0+1}{1+1}.$$

Likewise

$$\frac{1}{3} = \frac{0}{1} \pm \frac{1}{2} = \frac{0+1}{1+2} \quad \text{and} \quad \frac{2}{3} = \frac{1}{2} \pm \frac{1}{1} = \frac{1+1}{2+1}.$$

The result is always a rational number that lies between the original pair of rationals. Continuing in this manner, the infinite Farey tree is shown in Fig. A1. Notice the zig-zagging sequence of rationals with numerators and denominators from the Fibonacci sequence: 0/1, 1/2, 1/3, 2/5, 3/8, 5/13, ... These are the convergents of the continued fraction expansion of $1/\tau^2$ where $2\pi/\tau^2 = 137.5$ deg. is the principal divergence angle. The fact that they zig-zag along successive rows of the Farey tree signifies that the indices of their continued fraction expansion ends in a sequence of 1's,

$$1/\tau^2 = \left[2, \overline{1}\right] = 1/2+1/1+1/1+1\ldots$$

where the superscripted bar refers to a periodic sequence of indices. Successive convergents, again, have $M = \pm 1$.

The next most prevalent divergence angle found in phyllotaxis is given by the continued fraction: $[3, \overline{1}]$ with the sequence of convergents: 0/1, 1/3, 1/4, 2/7, 3/11, ... Note that the numerators follow a Fibonacci sequence while the denominators follow a Lucas sequence. These fractions approach $(0+1\tau)/(1+3\tau)$ along another zig-zag path, corresponding to the most prevalent divergence angle, 99.5 deg, of abnormal phyllotaxis.

KAPPRAFF (2002) has shown that the Farey tree is a graphical representation of the entire structure of all continued fractions. Beginning with 0/1 in the first row and 1/1 in the second row, the sequence of indices of the continued fraction describes how many rows in the Farey tree to descend in a RLRLRL ... zig-zag sequence to find the next convergent

which is always the nearest rational to the preceding one, in that row. For example, referring to Sequence (A2) leading to the continued fraction expansion of 17/47= [2134], the first convergent, 1/2, is found two rows beneath 0/1 and the right (R); 1/3 is one row below 1/2 and to the left (L); 4/11 is three rows beneath 1/3 and the right (R); ending with 17/47 four rows beneath 4/11 and to the left (L).

The class of divergence angles found in phyllotaxis are characterized by continued fractions whose convergents, after some point, zig-zag row by row. I have called the angles corresponding to these continued fractions, *noble angles*. They are characterized by the continued fractions of $(p_0+p_1\tau)/(q_0+q_1\tau)$ where p_0/q_0 and p_1/q_1 are the first two convergents of the continued fraction before the indices become 1's.

Figure 5b shows the left half of the Farey tree with the noble angles to which various sequences of phyllotaxis convergents approach. The rational fractions p/q correspond to the phyllotaxis numbers p, q.

Appendix B. The Golden Mean and Optimal Spacing

The ability of τ to evenly distribute numbers can be seen by observing the first 103 decimal places of Adamson's *Golden Ratio Phyllotaxis Constant* (GRPC):

.628407395174062851739528406395173062841739518406295173962840739517406284173952840629517306284073951844062 ...

A first glance might lead you to believe that the sequence .6284073951740 ... is repetitious, but a closer examination of the number reveals a long-term, non-periodic structure with only local repetitions. Exhibiting the digits as follows reveals interesting Fibonacci properties:

Lengths of sequences beginning with "6":

13 units Golden Ratio Phyllotaxis
13 Constant arranged in "6"
8 columns
13
8 Data at left - shows that up to
13 the first 103 digits, the GRPC
13 number can be grouped by
8 Fibonacci number of sequences
13 beginning with 6.

This series follows the pattern of the rabbit sequence (see Appendix D). As you can easily discover, a similar situation exists for each digit.

How is GRPC computed? To some extent it is analogous to Wythoff's game (see Appendix C), except that the decimal part of multiples of $1/\tau$ and $1/\tau^2$ are extracted instead of the integer parts. Multiply $1/\tau = 0.618$ ... successively by the integers, discard the integer part and extract the first number after the decimal point. This yields the GRPC. For example, $12/\tau = 7.416$ ... Therefore the 12th number in GRPC is 4. The complement of

GRPC, 0.3715926048, is generated by multiples of $1/\tau^2$, and GRPC and its complement sum to 1.000 ... just as $1/\tau$ and $1/\tau^2$ do. Some properties of GRPC are:

1. Differences between each digit are maximized: 4, 6, 4, 4, 4, 7, 4, 6 ...
2. The number is transcendental and has long-range aperiodicity.
3. It is easy to calculate any digit (unlike pi).
4. It has a long range *equitable distribution* and frequency of each digit 0 through 9: First 103 digits of the GRPC have 11-0's, 10-1's, 10-2's, 10-3's, 11-4's, 10-5's, 10-6's, 11-7's, 10-8's and 10-9's.

Appendix C. Wythoff's Game

My own interest in the fascinating world of Fibonacci numbers began as the result of playing *Wythoff's game* with my students at the New Jersey Institute of Technology KAPPRAFF (1986). This game is played as follows:

> Begin with two stacks of tokens (pennies). A proper move is to remove any number of tokens from one stack or an equal number from both stacks. The winner is the person removing the last token.

The winning strategy is based on Theorem C1 due to S. Beatty.

Theorem C1: If $1/x + 1/y = 1$, where x and y are irrational numbers, the sequences $[x]$, $[2x]$, $[3x]$, ... and $[y]$, $[2y]$, $[3y]$, ... together include every positive integer taken once ([ ] means "integer part of", e.g., [3.14] = 3).

For a proof, see COXETER (1953). Since $1/\tau^2 + 1/\tau = 1$, Beatty's theorem shows that $[n\tau]$, $[n\tau^2]$ exhausts all of the natural numbers with no repetitions, as n takes on the values $n = 1, 2, ...$ Table C1 shows results for $n = 1, 2, ..., 6$. Do you notice a pattern in these number pairs that enables you to continue the table without computation? These *Beatty* pairs are also winning combinations for Wythoff's game. At any move a player can reduce the number of counters in each stack to one of the pairs of numbers in Table C1. The player who does this at each turn is assured victory.

This sequence follows a rather subtle pattern. The differences between the numbers in each column are:

Table C1. Winning combination of Wythoff's game.

n	$[n\tau]$	$[n\tau^2]$
1	1	2
2	3	5
3	4	7
4	6	10
5	8	13
6	9	15

2 1 2 2 1 2 ... and 3 2 3 3 2 3 ...

Although both of these sequences follow a similar pattern (with 2 and 1 replaced by 1 and 0, respectively, in the first sequence, and 3 and 2 replaced by 1 and 0 in the second sequence):

101101011011011 ... (C1)

This is the so-called rabbit sequence because it relates to the famous problem posed by Fibonacci concerning the propagation of rabbits. This sequence is discussed in Appendix D. Adamson's Wythoff Wheel is shown in Fig. C1. The Wythoff pairs are placed in adjacent cells with the left hand column of integers labeled with 1's and the right hand column with 0's. Notice that the rabbit sequence is developed by the sequence of 0's and 1's in each concentric circle.

Appendix D. Zeckendorf Notation and the Rabbit Sequence

Figure D1 shows a tree graph depicting the growth of rabbits described by Fibonacci in his book *Liber Abac*: (1209).

> Each month a mature pair of rabbits gives birth to a pair of rabbits of opposite sex. However, a newborn rabbit pair must wait two months before it matures.

The branches in Fig. D1 are labeled in Fig. D2 in such a way that the branches representing the mature rabbits are labeled with a 1, while young rabbit branches get a 0.

This numbering system is a way to represent all the integers in a golden mean *decimal system* known as *Zeckendorf notation*. The elements of the Fibonacci tree are numbered in Zeckendorf *notation* beginning with the root labeled by a 1. Beginning with the root, follow

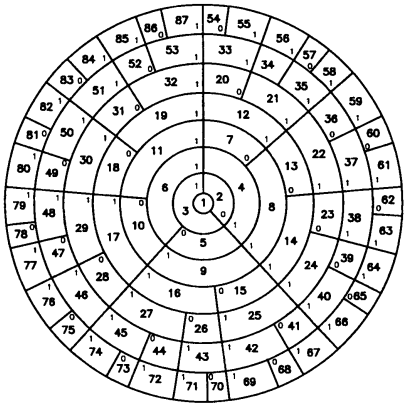

Fig. C1. Adamson's Wythoff Wheel. Adjacent number pairs are safe combinations for Wythoff's game.

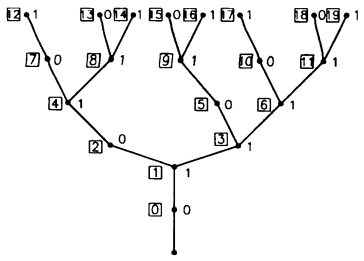

Fig. D1. The branches of the Fibonacci tree are labeled with a 1 for mature rabbits and 0 for young rabbits. This tree is the basis of a Fibonacci number system (Zeckendorf notation).

Table D1. Binary and Fibonacci representations of number.

	168421			85321	
0	0	0	0		
1	1	1	1	1	1
2	10	2	10	2	2
3	11	1	11	1	3
4	100	3	101	3	4
5	101	1	110	2	5
6	110	2	111	1	6
7	111	1	1010	4	7
8	1000	4	1011	1	8
9	1001	1	1101	3	9
10	1010	2	1110	2	10
11	1011	1	1111	1	11
12	1100	3	10101	5	12
13	1101	1	10110	2	13
14	1110	2	10111	1	14
15	1111	1	11010	4	15
16	10000	5	11011	1	16
17	10001	1	11101	3	17
18	10010	2	11110	2	18
19	10011	1	11111	1	19

the unique path to any element of the tree. The Zeckendorf representation of that number is given by the string of 0's and 1's along that unique path. For example, the number 13 is represented in this system by:

$$13 = 10110.$$

If each digit from right to left is weighted respectively according to the F-sequence, i.e., 1, 2, 3, 5, 8, 13, ..., and the Fibonacci numbers corresponding to the digits represented by 1's are added, the numbers on the branches of the Fibonacci tree are the succession of

integers, e.g., 101 = 3 + 1 = 4, 110 = 3 + 2 = 5, 111 = 3 + 2 + 1 = 6, 1010 = 5 + 2 = 7, 11010 = 2 + 5 + 8 = 15 ... The integers from 1 to 19 are listed in Table D1, along with their binary representations.

Notice the sequence that makes up the last digit or 1's column. It is the rabbit sequence:

$$101101011011011 \ldots \tag{D1}$$

This is the same sequence that we encountered in each column of Wythoff's sequence (see Appendix C) given by Sequence (C1). This pattern of numbers also makes up the 2's column except that in place of a 1, two 1's appear. The pattern also appears in the 3's column with three 1's replacing each 1 and two 0's in place of each 0; in the 5's column, five 1's replace each 1 while three 0's replace each 0.

The rabbit sequence is generated by beginning with 1 and successively replacing $1 \rightarrow 10$ and $0 \rightarrow 1$ to yield the sequence: 1, 10, 101, 10110, 10110101, 1011010110110, etc. Notice in this sequence that up to position F_n, the n-th Fibonacci number, in the sequence there are F_{n-1} 1's and F_{n-2} 0's where $F_1 = 1$, $F_2 = 1$, $F_3 = 2$, $F_4 = 3$, $F_5 = 5$, $F_6 = 8$, ... For example up to the 5th position there are three 1's and two 0's. KAPPRAFF (2002) has shown that this sequence provides the symbolic dynamics of a dynamical system known as the circle map at the brink of chaos.

The numbers in Table 1D to the right of the binary and Zeckendorf notation represent the digit numbered from the right in which a 0 changes to a 1 between successive integers. They form two sequences,

$$\text{TOH Sequence: } 1213121412131215121 \ldots \tag{D2}$$

$$\text{TOH-Fibonacci Sequence: } 1213214132152141321 \ldots \tag{D3}$$

Sequence (D2) is the sequence of moves for the well-known Tower of Hanoi puzzle (TOH) described with great detail in KAPPRAFF (2002). Series 3D is the analogous sequence for the Fibonacci system. These sequences are full of number patterns. For example, the 1's from the binary sequence follow each other after every 2 spaces. In other words it is periodic. In the rabbit sequence the 1's follow each other according to the sequence 232332 ..., which is the rabbit sequence if 2 is replaced by 0 and 3 is replaced by 1. While the Sequence (D2) is periodic in each of its digits, Sequence (D3) is almost periodic, or *quasiperiodic* as mathematicians say. You can check the comparable patterns within both sequences for the numbers 2, 3, 4, 5.

It is interesting to note that the sequence of moduli between successive rationals in each row of the infinite Farey tree in Fig. A1 follows the pattern: 3, 353, 3537353, 353735393537353, ... If 3, 5, 7, 9, ... is replaced by 1, 2, 3, 4, ...the TOH sequence is developed as shown in Sequence (D2).

REFERENCES

ADLER, I. (1997) Generating phyllotaxis patterns on a cylindrical point lattice and Prologue, in *Symmetry of Plants* (eds. R. V. Jean and D. Barabe), World Scientific, Singapore.

COXETER, H. S. M. (1953) Golden mean phyllotaxis and Wythoff's game, Scripta Mathematica, XIX(2,3).
COXETER, H. S. M. (1962) *Introduction to Geometry*, Wiley, New York.
ERICKSON, R. O. (1983) The geometry of phyllotaxis, in *The Growth and Functioning of Leaves* (eds. J. E. Dale and F. L. Milthorpe), pp. 54–88, Cambridge Univ. Press, New York.
KAPPRAFF, J. (2002) *Mathematics Beyond Measure: A Guided Tour through Nature, Myth, and Number*, World Scientific, Singapore.
KAPPRAFF, J., BLACKMORE, D. and ADAMSON, G. W. (1997) Phyllotaxis as a dynamical system: a study in number, in *Symmetry of Plants* (eds. R. V. Jean and D. Barabe), World Scientific, Singapore.
KIMBERLING, C. (A054065) In On-Line Encyclopedia of Integer Sequences, Neil J. A. Sloane, editor-in-chief.
MARZEC, C. and KAPPRAFF, J. (1983) Properties of maximal spacing on a circle related to phyllotaxis and to the golden mean, *J. theor. Biol.*, **103**, 201–226.
PRUSINKIEWICZ, P. and LINDENMYER, A. (1990) *The Algorithmic Beauty of Plants*, Springer Verlag, New York.
VAN ITERSON, G. (1907). *Mathematische and Mikroskopish-Anatomische Studien uber Blattstellungen*, Gustav Fischer, Jena.